energies

Article

Economic and Energetic Assessment and Comparison of Solar Heating and Cooling Systems

Boris Delač , Branimir Pavković * and Vladimir Glažar

Department of Thermodynamics and Energy Engineering, Faculty of Engineering, University of Rijeka, Vukovarska 58, 51000 Rijeka, Croatia
* Correspondence: branimir.pavkovic@riteh.hr

Abstract: Solar heating and cooling (SHC) systems are currently attracting attention, especially in times of increasing energy prices and supply crises. In times of lower energy prices, absorption SHC systems were not competitive to compression cooling supported by photovoltaic (PV) modules due to the high investment costs and total energy efficiency. This paper aims to discuss the current changes in energy supply and energy prices in terms of the feasibility of the application of a small absorption SHC system in a mild Mediterranean climate. The existing hospital complex restaurant SHC system with evacuated tube solar collectors and a small single-stage absorption chiller was used as a reference system for extended analysis. Dynamic simulation models based on solar thermal collectors, PV modules, absorption chillers and air-to-water heat pumps were developed for reliable research and system comparison. The results showed that primary energy consumption in SHC systems designed to cover base energy load strongly depends on the additional energy source, e.g., boiler or heat pump. Absorption SHC systems can be price competitive to air-to-water heat pump (AWHP) systems with PV collectors only in the case of reduced investment costs and increased electricity price. To reach acceptable economic viability of the absorption SHC system, investment price should be at least equal to or lower than a comparable AWHP system.

Keywords: solar heating and cooling; absorption chiller; heat pump; simulation

Citation: Delač, B.; Pavković, B.; Glažar, V. Economic and Energetic Assessment and Comparison of Solar Heating and Cooling Systems. *Energies* **2023**, *16*, 1241. https://doi.org/10.3390/en16031241

Academic Editor: Mirko Morini

Received: 19 December 2022
Revised: 12 January 2023
Accepted: 18 January 2023
Published: 23 January 2023

1. Introduction

Current environmental policy is becoming rigorous regarding primary energy consumption, while energy demands are increasing due to higher requirements for thermal comfort. In such conditions, renewable energy sources and energy-efficient systems are necessary for sustainable development. The year 2020 represented a milestone for the renewable energy sector, as it was the deadline for reaching the targets from the Renewable Energy Directive of 2009. As expected, based on the slow evolution over the years, most countries failed to reach their indicative targets for solar heating and cooling [1].

With technology developments and increased application, followed by reduced equipment costs, the utilization of solar energy became interesting for integration into heating and cooling (H/C) systems by the integration of solar thermal collectors (STC) or photovoltaic (PV) modules. Presently, installed solar thermal heating equipment in Europe generates an estimated 27 TWh of energy for heating [2]. Some applications such as solar cooling still show a questionable level of feasibility and must be carefully considered in design if any acceptable level of cost efficiency is expected, which is more important to investors than environmental issues. By the end of 2015, only 1350 solar cooling systems were installed worldwide [3]. In 2018, the number of installed solar thermal cooling systems increased to 1800, and it is estimated that the number of installations surpassed 2000 in 2021 [4]. This number is still negligible when compared to widely applied compression cooling systems. The most probable explanation for such a situation is that cost-related feasibility problems with those installations are present everywhere. In general, both PV-and ST-driven system feasibility is investment dominated. The focus in development, especially for small-scale systems, needs to be on the reduction of the initial investment, making it simple and compact [5].

Most of the research on small-scale solar cooling systems is based on a system with evacuated tube solar collectors and a single-stage absorption chiller (ACH) [6–12]. The performance of these systems is often compared to conventional heating or cooling generators with fossil fuel or electricity to estimate primary energy savings and economic benefits [7,8,13–17] or environmental impact [7,9]. Sizing the absorption chiller for covering only a fraction of the design load leads to better economic indicators [6,9,11,17,18]. Thereby, it is also possible to achieve more operating hours with the chiller working at maximal load and thus less electrical energy consumption by auxiliary equipment required to run the system.

Some of the first estimations of solar absorption cooling systems were carried out by Florides et al. [14,15] who concluded that the system could provide environmental and economic benefits in comparison with a conventional system based on an oil boiler and vapor compression chiller, but the limitation is high investment costs for the chiller. Ma et al. [19] conducted numerical research on the feasibility of different solar-assisted air conditioning systems for office buildings in Australia. The study confirmed the energy efficiency of systems without economic benefits. The key point in achieving the economic feasibility of solar cooling systems is reduction of the initial cost. Huang et al. [20] evaluated the annual operation of solar thermal heating and absorption cooling systems with additional air-source heat pumps installed in China. The authors determined energy efficiency and annual electricity savings of more than 40% of the total electricity consumption for building cooling and heating. Figaj and Zoladek [21] performed an energy and economic assessment for a solar heating and cooling (SHC) system for a household building. The system comprised solar thermal collectors coupled with a reversible heat pump and an absorption or adsorption chiller. The authors determined economic viability for the system located in the warm climate of Naples with a payback period of up to 12 years, while the proposed system is not viable in the colder climate of Krakow, since a payback period of 20 years is achieved. Arsalis and Alexandrou [16] concluded that the SHC system has favorable running costs in comparison with an air-to-water vapor compression heat pump, but their estimations did not include auxiliary equipment electricity consumption, maintenance costs, or consumption and cost for water supplied to cooling towers due to evaporation. Kaneesamkandi et al. [22] compared the absorption SHC system and vapor compression cooling system in the climatic zones of Niger, Riyadh and Beijing. They concluded that the absorption SHC shows an advantage in electricity consumption and emissions, but for better overall performance, additional cost reduction of equipment is required. Lazzarin et al. [23] performed an energy analysis for the variety of solar thermal and ground source absorption heat pump systems combined with an air-to-water chiller for heating and cooling of an educational building located in Northern Italy. The authors concluded that all the considered systems are energy efficient, but for reaching economic viability, an incentive of 65% of the investment cost is required.

The analyzed literature and the cited literature also show that the investment price for SHC systems often includes only the cost of the equipment, without the installation cost or any other unpredicted cost that may be incurred during the project implementation. Small-scale chillers are considered in different price ranges: lower ones at 400–500 EUR/kW [14,15,19], 1000–1500 EUR/kW [17,23] and 1500 EUR/kW [16], and higher ones at 2000–2600 EUR/kW [8]. The general impression of the authors of the present paper based on long-term experience with HVAC system design and construction is that those values are underestimated and could lead to misleading conclusions about the economic viability of these systems.

The cited papers based on dynamic system simulations differ considerably in the details of the simulation models. In many of them, the authors have considered only simple system configurations with no control system and without precisely presented design parameters. In some papers, the authors have neglected important components of the SHC system, such as heat rejection from the condenser and absorber, which has a strong impact on the system's efficiency. The possibility of improving the energy efficiency of existing absorption SHC systems by expanding solar thermal energy use or using the waste heat from the condenser and absorber for heating purposes was also not considered in the papers reviewed in this study. Due to the current energy crisis, supply interruptions caused an increase in equipment prices, and with an increase in energy prices, the situation has changed, and new cost analyses of existing technologies are welcome.

In this paper, different configurations of absorption SHC systems are compared with systems based on compression heat pumps supported by photovoltaic (PV) modules. Dynamic simulation models for buildings and HVAC systems in a mild Mediterranean climate are developed for reliable investigations. A full economic and energy evaluation of the system operation during its lifetime is performed. The study takes into account current changes in energy supply by including different price scenarios.

2. Materials and Methods

2.1. Energy

The following case study analysis is intended to compare the energetic and economic indicators of SHC systems. Energetic indicators comprise primary energy consumption, renewable energy share and the insight into the possibility to make the system completely renewable by covering nonrenewable energy share in system electric energy consumption. The analysis covered only building HVAC systems, which means that other energy consumption of the building (e.g., lighting, appliances, etc.) was not included in the consideration.

Energy consumption of each energy carrier in an HVAC system $E_{\text{cons,i}}$ can be estimated by numerical dynamic simulation of the system or by experimental measurements. In the case when the system is equipped with its own energy production system, the energy that is imported to the system $E_{\text{imp,i}}$ is calculated by deduction of consumed energy $E_{\text{cons,i}}$ with produced energy $E_{\text{prod,i}}$:

$$E_{\text{imp,i}} = E_{\text{cons,i}} - E_{\text{prod,i}} \tag{1}$$

Primary energy consumption E_{P} is calculated for imported energy to the system by using nonrenewable energy factor $f_{\text{nren,i}}$ for each carrier of imported energy:

$$E_{\text{P}} = \sum_{i} \left(E_{\text{imp,i}} \cdot f_{\text{nren,i}} \right) \tag{2}$$

Primary energy consumption indicator PEC is derived by dividing primary energy consumption with net usable building area.

$$PEC = E_{\text{P}}/A \tag{3}$$

Fossil fuels are nonrenewable and do not contain renewable energy. However, electricity, depending on the production process and sources, can contain both forms of energy, and the situation differs from country to country. The share of nonrenewable energy ($f_{\text{ee,nren}}$) for Croatia [24] and Eurostat data [25] were used to evaluate the nonrenewable part of consumed electricity from self-produced and imported shares of electric energy in Croatia—totaling 50% ($f_{\text{ee,nren}}$ = 0.5).

$$E_{\text{cons,ee,nren}} = E_{\text{cons,ee}} \cdot f_{\text{ee,nren}} \tag{4}$$

A PV system that generates renewable energy necessary to cover the nonrenewable part of consumed electricity added to the HVAC system can in some way help to make the entire building energy system carbon neutral.

$$E_{\text{prod,ee}} > E_{\text{cons,ee,nren}} \tag{5}$$

Renewable energy share RES in consumed energy is determined as

$$RES = \sum_i E_{\text{cons,res}} / \sum_i E_{\text{cons,i}} \tag{6}$$

The fraction of cooling energy produced by the absorption chiller $E_{\text{C,ACH}}$ in total produced energy for cooling a building E_{C} is calculated as:

$$ACF = E_{\text{C,ACH}} / E_{\text{C}} \tag{7}$$

The solar fraction in total produced energy for heating is calculated as:

$$SF_{\text{i}} = E_{\text{SOL,i}} / E_{\text{H,i}} \tag{8}$$

where $E_{\text{SOL,i}}$ is useful energy from solar collectors transferred to the heating subsystem (e.g., for DHW heating or building heating), and $E_{\text{H,i}}$ is total energy produced for the heating subsystem.

2.2. Costs

The global cost contains investment, operating and maintenance costs. By applying the discount rate using a discount factor, global costs are expressed in terms of value in the starting year:

$$G_g(\tau) = G_I + \sum_j \left[\sum_{i=1}^{\tau} (G_{a,i}(j) \cdot R_d(i)) - V_{f,\tau}(j) \right] \tag{9}$$

where τ is the calculation period, C_{I} is the initial investment cost for the HVAC and PV system, C_{a} is the annual operating cost multiplied by R_{d}, which is the average discount factor calculated for each year of the evaluation period, and $V_{\text{f},\tau}$ is the average residual value at the end of the evaluation period. This calculation procedure is repeated for each year of the calculation period. The discount factor is calculated as:

$$R_{\text{d}}(p) = [1/(1 + \text{r}/100)]^p \tag{10}$$

where p is the number of years from the starting period, and r is the real discount rate.

The indicator of global cost CI is derived by dividing global cost G_{g} by net usable building area A.

$$CI = G_{\text{g}} / A \tag{11}$$

2.3. Case Study—The Building

The building considered in this paper is located in a complex of a special hospital in Crikvenica, Croatia. The building has three floors, but the presented analysis is performed for the restaurant area, which is located on the first floor of the building. The conditioned space is separated into three dining halls with a total surface of 530 m^2. The building was constructed in the first half of the 20th century using materials typical of that period and massive construction. The main characteristics of the building are listed in Table 1.

Using the geometry and building properties, the multizone model was created in Google SketchUp with the Trnsys3d plugin, which was later imported into the TRNSYS environment as a Type 56 thermal model. Figure 1 shows the building and the first floor where the restaurant is located. The model consists of 7 thermal zones: 3 zones represent the restaurant dining area while the rest of the zones represent the surrounding unconditioned space. To achieve shorter simulation runtime with a sufficient level of accuracy, the thermal zones on floors above and below the modeled area were not modeled but were considered as a conditioned space with the corresponding temperature as a boundary condition of the building elements adjacent to these floors.

Table 1. Main characteristics of the building regarding physics, operation, and climate data.

Climate data	City	Crikvenica (Croatia)
	Longitude	14.6915 E
	Latitude	45.1736° N
Physics	Dimensions (length x width x height)	$36 \times 21 \times 3.2$ m
	Conditioned area	756 m^2
	Conditioned volume	2419 m^3
Envelope	External wall *U*-value	0.85 W/m^2 K
	Internal wall *U*-value	0.9 W/m^2 K
	Ceiling/floor towards the building *U*-value	0.75 W/m^2 K
	Floor on the ground *U*-value	1.93 W/m^2 K
	Window/door *U*-value	2.9 W/m^2 K
Ventilation	Infiltration/required ventilation rate	0.42 h^{-1}/5.62 h^{-1}
	Mechanical ventilation	Not existing
Occupancy and operation	Occupancy	7 days in a week 8–10 AM 12 AM–2 PM 6 PM–9 PM
	Number of persons	200 persons
	Internal heat gains	6 W/m^2
	Heating and cooling operation	Interrupted 7 AM–9 PM
	Heating temperature set point	22 °C
	Cooling temperature set point	24 °C
	DHW set point	45 °C

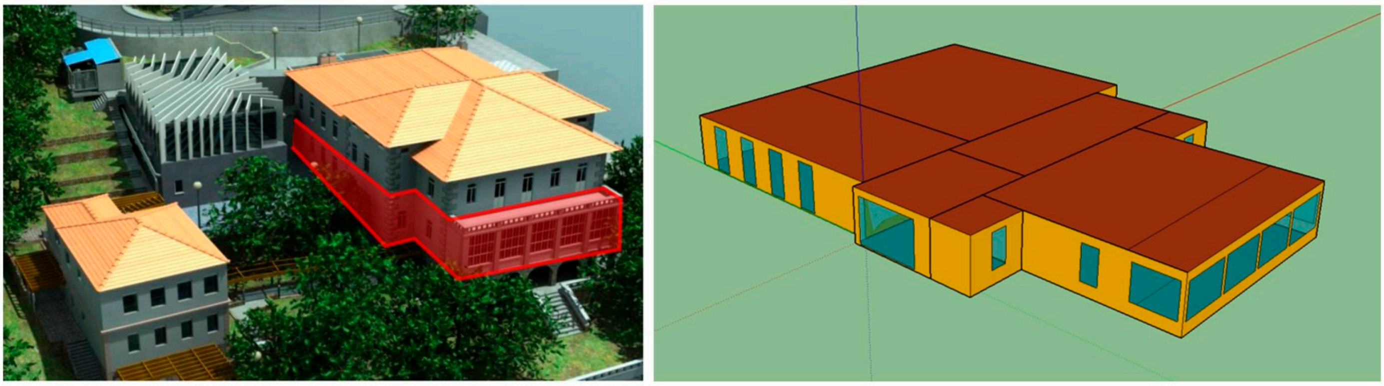

Figure 1. The building with the restaurant area considered in the case study is marked in red (**left**) and a 3D thermal model of the restaurant area (**right**).

Daily occupancy and operating conditions were acquired from the employed staff. The restaurant operates 7 days per week from 7 AM to 9 PM, with peak occupancy from 8 to 10 AM, 12 AM to 2 PM and from 6 to 9 PM. The spaces are conditioned with interrupted operation outside working hours. The set point temperature is 22 °C for the heating period and 24 °C for the cooling period. The dining area does not have a mechanical ventilation system, but ventilation during operating hours is accounted for by the required number of air changes per hour and infiltration during non-operating hours [26].

The energy consumption for H/C is calculated by performing the annual energy simulation under the meteorological boundary conditions of a synthetic test reference year (TRY), created for the nearest referent meteorological station of the building considered in this work (Senj, Croatia). A synthetic TRY with a time step of one hour was created using the software Meteonorm [27]. The new dataset had the same statistical properties as the available monthly minimum, maximum and average values provided by the Croatian Meteorological and Hydrological Service [28]. Figure 2 shows the annual variation of ambient temperature, relative humidity, and solar radiation on the horizontal surface.

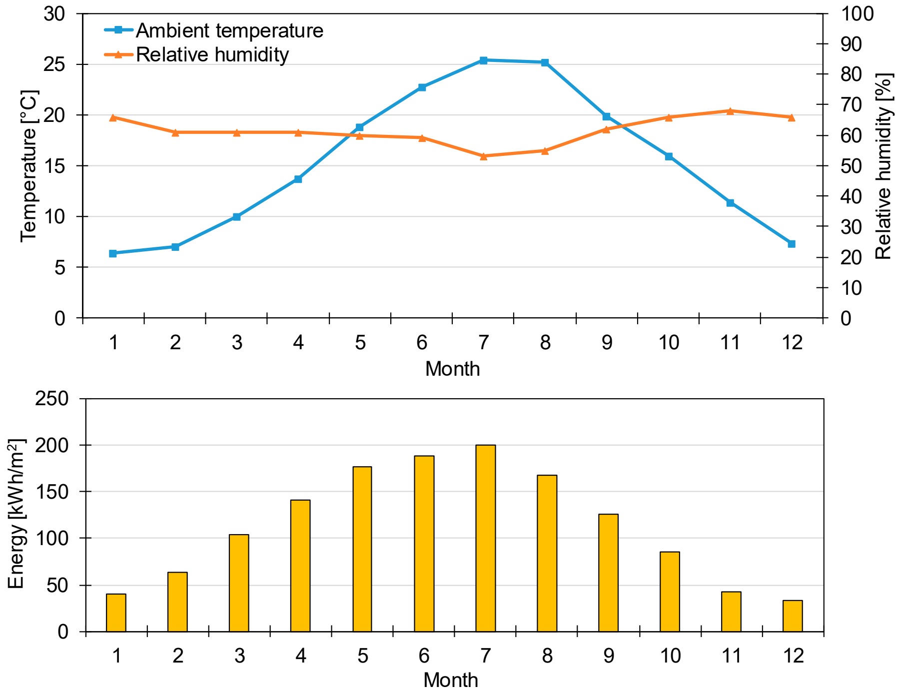

Figure 2. Annual variation of mean monthly ambient temperature and mean monthly relative humidity (**upper**); annual variation of monthly solar radiation on a horizontal surface (**lower**).

The consumption of thermal energy for H/C in the building calculated using the simulation is shown in Figure 3. The total energy consumption for heating the building is 27,938 kWh (37 kWh/m^2), and the energy for cooling is 12,015 kWh (16 kWh/m^2). Figure 3 shows that partial loads prevail during the year. The design load for building heating of 45 kW was calculated according to the methodology proposed in EN 12831 [29]. The design load for building cooling of 35 kW was calculated using the calculation procedure from VDI 2078 [30]. The design loads were calculated for interrupted H/C operation, and the results are shown in Figure 4. The cooling load was strongly affected by the heat gains of the occupants. The peak values of the required cooling load occurred during the periods that coincided with the occupancy of the dining halls.

The energy generated by a centralized hydronic system for heating and cooling is distributed to fan coils in the restaurant. All systems have the same water temperature, which is 50/45 °C for heating and 7/12 °C for cooling. Central heating of DHW is provided in the building, and therefore, it is included in all the systems. Cold water is heated from a temperature of 12 to 45 °C. DHW consumption was monitored in the period from January 2017 to December 2018. Daily consumption varied from 1800 to 2600 L/day. According to [31], DHW consumption equaled the range of 12 to 30 L/person/day at the temperature of 45 °C; thus, the measured values are in accordance with those from the literature. The monitored data are used to the create a consumption profile for a standard day in a year, as shown in Figure 5.

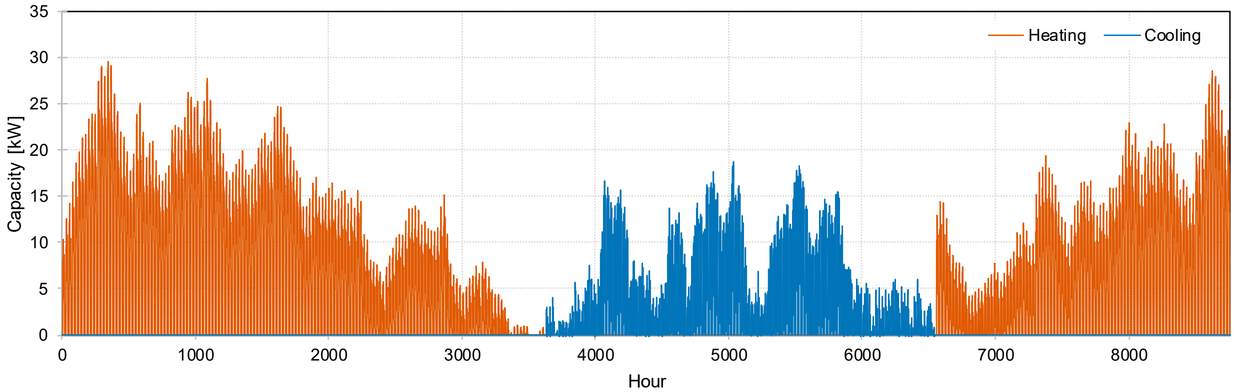

Figure 3. Useful energy for heating and cooling calculated for location Senj (TRY).

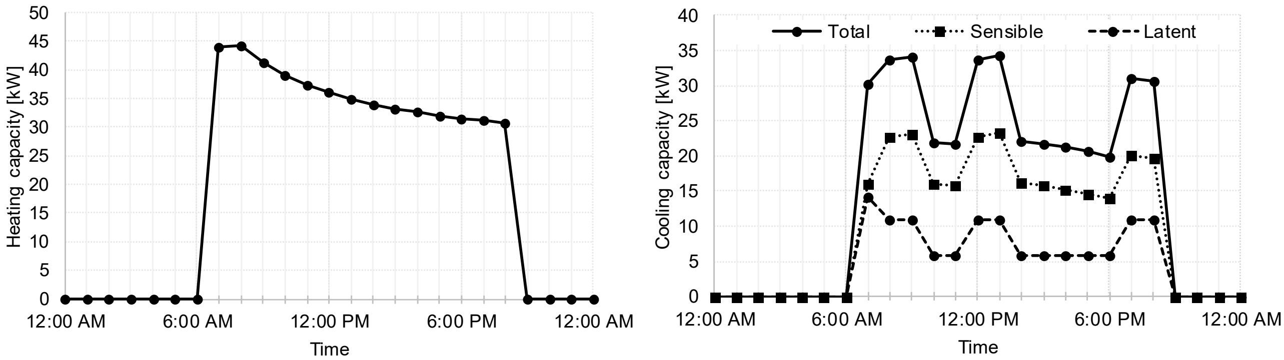

Figure 4. Daily variation of design load for heating (**left**) and cooling (**right**).

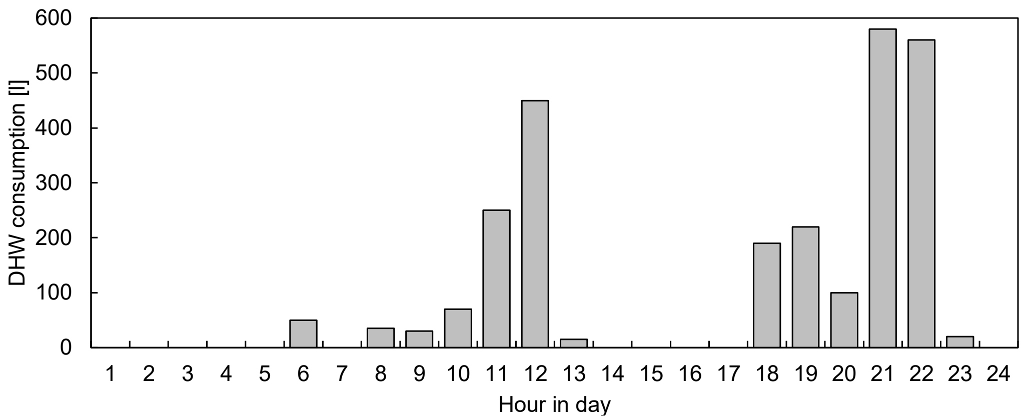

Figure 5. DHW consumption profile for a standard day in a year.

2.4. Building Energy Systems

The research is conducted on different HVAC systems based on SHC technologies. The systems are listed in Table 2 with technologies used for building H/C, DHW heating, and electricity production if available.

Table 2. HVAC systems considered in the analysis.

System	Building Heating	Building Cooling	DHW Heating	Electricity Production
S-FO-ACH-1	Fuel oil boiler	ACH * Split AC *	Fuel oil boiler STC *	-
S-FO-ACH-2	Fuel oil boiler STC *	ACH * Split AC *	Fuel oil boiler STC *	-
S-NG-ACH-1	Natural gas boiler	ACH * Split AC *	Natural gas boiler STC *	-
S-NG-ACH-2	Natural gas boiler STC *	ACH * Split AC *	Natural gas boiler STC *	-
AWHP-1	AWHP *		AWHP *	-
AWHP-2	AWHP *		AWHP *	PV

* STC—solar thermal collectors, ACH—absorption chiller, split AC—split type air conditioner, AWHP—air-to-water heat pump.

2.4.1. S-FO-ACH-1/S-NG-ACH-1 System

The solar absorption cooling and heating system are installed in the presented building as one of the demonstration pilot plants that were designed and set up in the Adriatic region to gain better insight into the operation of these systems. This system is considered in the variant where the energy for heating is generated by the fuel oil boiler SL-FO-ACH-1 and the variant with the natural-gas-fired boiler S-NG-ACH-1. Both systems based on absorption cooling have in common evacuated tube solar collectors and a single-stage LiBr–H_2O absorption chiller. The system is presented in Figure 6. The solar system consists of four groups of evacuated tube collectors with a 52 m^2 total absorber area facing south at an inclination of 35°. A propylene glycol-based mixture medium was chosen as the heat transfer fluid to prevent freezing in the solar system during winter. Hot-water-driven single effect LiBr–H_2O absorption chiller supplies chilled the water to the fan coils. The nominal cooling capacity is 17.5 kW with water temperatures of 12.5/7 °C at the evaporator, 88/83 °C at the generator and 31/35 °C at the condenser/absorber. Furthermore, 25.1 kW of hot water energy is required to run the chiller, while 42.7 kW of waste heat is rejected from the condenser and absorber by the wet cooling tower. Prior to installing the SHC system, split-type air conditioners with a total cooling capacity of 45 kW were used. These units were intentionally left in operation to allow for installments of ACH with a reduced capacity that will cover the base cooling load. During the cooling period, split-type air conditioners are set in operation with an air temperature set point for the restaurant at 26 °C. To ensure the prevalent operation of the SHC system for cooling, for utilizing the of thermal accumulation of massive buildings, and for less part load operation with high auxiliary power demand, the temperature set point for the fan coil operation is 22 °C.

An open-type cooling tower CT is used to reject heat from the absorber and condenser. Cooling water on its way to the cooling tower flows through the heat exchanger HX-2, which enables the utilization of waste heat for DHW preheating in storage tank S-2 with a volume of 2 m^3. The frequency controller is used to control the cooling tower fan speed while maintaining outlet water temperature in the range of 26–30 °C. Control valve RV-3 also provides the possibility either to control outlet temperature from the cooling tower by routing water from ACH to the cooling tower inlet or to bypass it. Chilled water from ACH is stored in tank S-4 with a volume of 1 m^3.

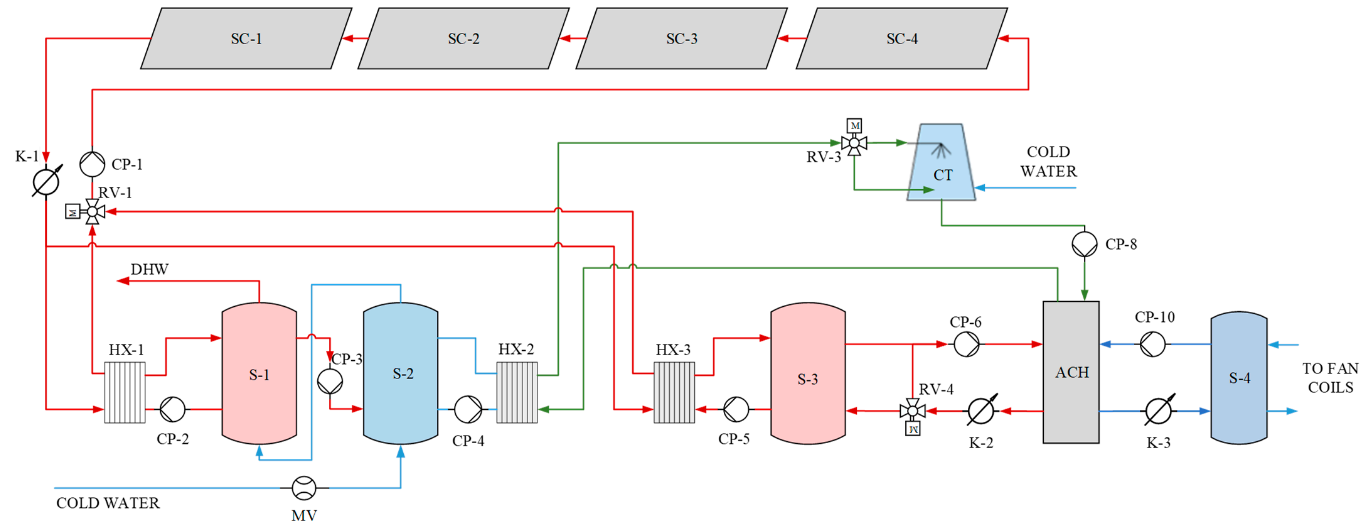

Figure 6. S-FO-ACH-1/S-NG-ACH-1—solar DHW heating and absorption space cooling system layout.

The solar collectors are hydraulically connected to heat exchangers HX-1 and HX-3. During the cooling season, by controlling valve RV-1, heat from the solar collectors is transferred to the heat exchanger HX-3 and hot storage tank S-3 for running the absorption chiller. If there is no need for cooling, the solar heat is used to preheat DHW; thus, it is transferred to the DHW storage tank S-1 (2 m^3 volume) via heat exchanger HX-1. DHW from storage tank S-1 is further distributed to three hospital wards and, if necessary, locally heated to 60 °C by a heat exchanger connected to a central hot water boiler.

2.4.2. S-FO-ACH-2/S-NG-ACH-2 System

Due to excess heat available from solar thermal collectors, a variant of the HVAC system with the utilization of solar heat for space heating is also considered. The system is presented in Figure 7. The solar collectors are hydraulically connected to heat exchangers HX-1, HX-3 and HX-4. Operation during the cooling season is the same as for the previously described solar absorption cooling system. During the heating season, by controlling valves RV-1 and RV-2, heat from the solar collectors is transferred to the heat exchanger HX-4, which heats the return water from the fan coils. If there is a need for heating supply water for building heating, the system is provided with heat exchanger HX-5, which is connected to a central hot water boiler (fired by fuel oil or natural gas).

2.4.3. AWHP-1 System

A simple schematic of the system with air-to-water heat pumps is presented in Figure 8. Two air-to-water heat pumps are provided in the system. A standard air-to-water heat pump (HP-1) operates during the year for heating DHW via heat exchanger HX-1. DHW is stored in tank S-1 with a volume of 2 m^3. The heating capacity of the unit is 28 kW at a condenser water temperature of 65/60 °C and an outside air temperature of −6 °C. COP at design conditions is 2.7.

A reversible air-to-water heat pump (HP-1) is intended for H/C in the building. The unit is sized to cover the design heating capacity at a 50/45 °C water temperature and outside air temperature of −6 °C (the selected unit has a heating capacity of 45 kW and COP 2.4). Design cooling capacity is supplied at an outdoor air temperature of 35 °C and an evaporator water temperature of 12/7 °C (the selected unit has a cooling capacity of 58.6 kW and EER 2.8). Inertial storage tank S-2 with a volume of 1 m^3 is provided in the system.

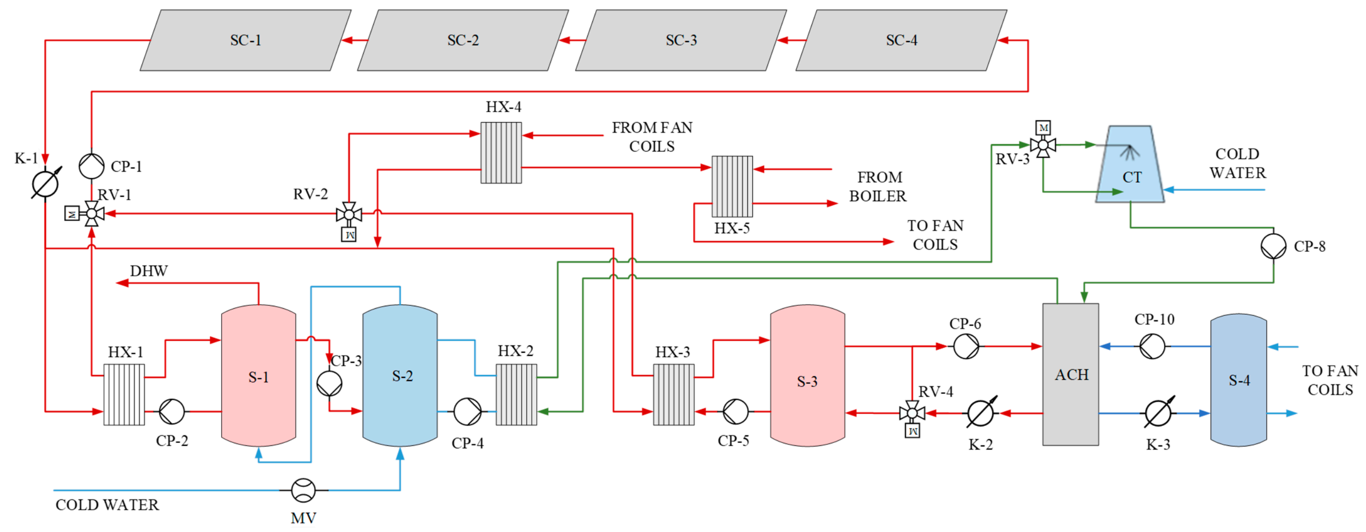

Figure 7. SL-FO-ACH-2/S-NG-ACH-2—solar space and DHW heating and absorption space cooling system layout.

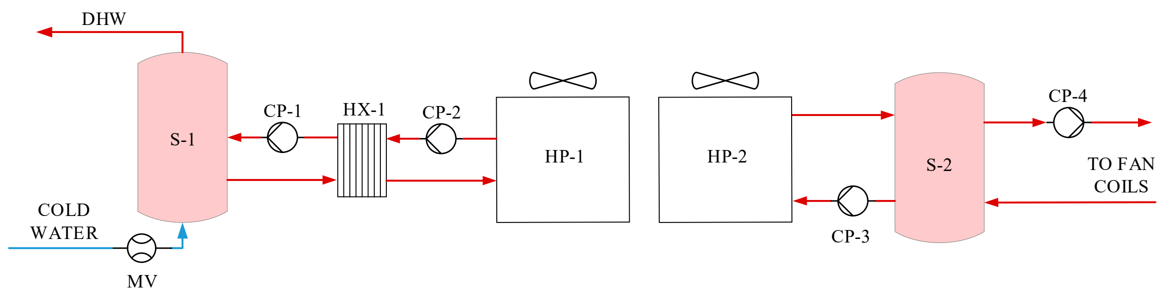

Figure 8. AWHP-1 and AWHP-2—air-to-water heat pump system for DHW heating, space heating and space cooling.

AWHP units are simulated using the model Type203 developed by the authors [32]. The model is based on the standard Trnsys AWHP model with the implementation of outlet water set point temperature and variable unit efficiency as a function of system temperatures and partial load efficiency.

2.4.4. AWHP-2 System

The AWHP-2 system is made by adding PV modules to the AWHP-1 system. The array size is determined by calculating the required amount of electricity to cover the nonrenewable part in the total electricity consumption required to run the H/C and DHW system during the year. Modules are placed into three arrays on the roof of the auxiliary building. The arrays are oriented toward the SW and are placed at an inclination of 20°. Each module has a total area of 3.25 m^2, which results in 0.6 kW of nominal power. The panels are monocrystalline with a declared efficiency of 18%. The PV system was simulated using the Trnsys model Type562d.

2.5. Costs

The research was conducted on the case study of HVAC systems located in Croatia; therefore, European Union guidelines [33,34] were applied for the calculation of total cost. The total cost was considered through investment, operating and maintenance costs. The calculation procedure was repeated for each year in a 15-year calculation period, which is defined for commercial nonresidential buildings.

2.5.1. Investment Cost

The investment cost is based on the costs of energy production systems (heating, cooling, electricity). SHC system costs include the cost of installation of H/C in the machine room and outside of the building (solar thermal collectors, cooling tower). There is no difference in investment cost between variants with fuel oil or natural gas boilers. AWHP system costs include the cost of installation of H/C equipment in the machine room and PV modules outside the building. The heat distribution and emission systems are the same for all systems. These costs are not considered to achieve more clear insight into the comparison of energy production systems. Procurement costs include investments for all major equipment. The cost of installation and associated works was estimated at 20% of the equipment procurement cost. Investment costs are presented in Table 3.

Table 3. Investment costs.

<table>
<tr><th>System</th><th>Description</th><th>Price</th></tr>
<tr><td rowspan="5">S-FO-ACH-1
or
S-NG-ACH-1</td><td>Solar thermal collectors, pipeline, pumps, valves, fittings, supporting construction</td><td>57,000 EUR</td></tr>
<tr><td>Absorption chiller, storage tanks, cooling tower, heat exchanger, pipeline, pumps, valves, fittings</td><td>66,000 EUR</td></tr>
<tr><td>DHW storage tanks, heat exchangers, pipeline, pumps, valves, fittings</td><td>15,000 EUR</td></tr>
<tr><td>Automation and wiring</td><td>43,000 EUR</td></tr>
<tr><td>Total</td><td>181,000 EUR</td></tr>
<tr><td rowspan="5">S-FO-ACH-2
or
S-NG-ACH-2</td><td>Solar thermal collectors, pipeline, pumps, valves, supporting construction, additional heat exchanger</td><td>58,000 EUR</td></tr>
<tr><td>Absorption cooling: chiller, storage tanks, cooling tower, heat exchanger, pipeline, pumps, valves, fittings</td><td>66,000 EUR</td></tr>
<tr><td>DHW storage tanks, heat exchangers, pumps, valves, fittings</td><td>15,000 EUR</td></tr>
<tr><td>Automation and wiring</td><td>43,000 EUR</td></tr>
<tr><td>Total</td><td>182,000 EUR</td></tr>
<tr><td rowspan="4">AWHP-1</td><td>Air-to-water heat pump for heating and cooling, inertial storage tank, pipeline, pump, valves and fittings</td><td>35,000 EUR</td></tr>
<tr><td>Air-to-water heat pump for DHW heating, DHW storage tank, heat exchanger, pumps, valves, fittings</td><td>25,000 EUR</td></tr>
<tr><td>Automation and wiring</td><td>20,000 EUR</td></tr>
<tr><td>Total</td><td>80,000 EUR</td></tr>
<tr><td rowspan="5">AWHP—2</td><td>Air-to-water heat pump for heating and cooling, inertial storage tank, pipeline, pump, valves and fittings</td><td>35,000 EUR</td></tr>
<tr><td>Air-to-water heat pump for DHW heating, DHW storage tank, heat exchanger, pumps, valves, fittings</td><td>25,000 EUR</td></tr>
<tr><td>Automation and wiring</td><td>20,000 EUR</td></tr>
<tr><td>PV plant (18 kW)</td><td>14,400 EUR</td></tr>
<tr><td>Total</td><td>94,400 EUR</td></tr>
</table>

2.5.2. Energy Cost

Prices for electricity, fuel oil, natural gas and water replenishment in cooling towers are presented in Table 4. The system operates from 7 AM to 9 PM; thus, the electricity price is considered only in the daily tariff. The fee for the engaged electric power is not charged in the considered tariff model. Due to the present energy crisis, electricity price is subsidized by the government. It can vary significantly, depending on the annual electricity consumption. Considering three different electricity prices, energy costs are evaluated in three scenarios.

Table 4. Energy prices.

Energy Carrier		Cost	Price
Electricity	Scenario S1	0.13	EUR/kWh
	Scenario S2	0.23	EUR/kWh
	Scenario S3	0.28	EUR/kWh
Fuel oil		0.118	EUR/kWh
Natural gas		0.057	EUR/kWh
Water		2.7	EUR/m^3

2.5.3. Maintenance Cost

The usual practice is to estimate the maintenance cost as a percentage of the investment cost. Absorption SHC systems have high investment costs, which are more than two times larger than the cost for AWHP systems. The consequence of this would be unrealistic maintenance costs and the cost advantage of AWHP systems. To prevent this, the maintenance cost for all the HVAC systems is estimated at a fixed amount of 2500 EUR per year. The maintenance cost for the PV system is estimated at 100 EUR/year, which includes cleaning of the module's surface once per year.

2.6. Primary Energy Consumption and CO_2 Emissions

Primary energy consumption is calculated from the final energy consumed by the system, and primary energy factors are defined at the national level for Croatia. CO_2 emissions are also calculated according to final energy consumption. Primary energy factors and emission factors used in the calculations are presented in Table 5.

Table 5. Primary energy factors and CO_2 emission factors.

Energy Source		Value	Unit
Electricity	Primary energy factor	1.614	-
	CO_2 emission factor	0.2348	kg/kWh
Fuel oil	Primary energy factor	1.138	-
	CO_2 emission factor	0.2995	kg/kWh
Natural gas	Primary energy factor	1.095	-
	CO_2 emission factor	0.2202	kg/kWh

3. Results

Year-round energy simulations are conducted for the building and HVAC systems presented in Section 2. Produced energy for building H/C, as well as DHW heating, separated into energy carriers, energy consumption and key performance indicators, are presented in Table 6.

Table 6. Results of HVAC system simulations represented by produced energy, consumed energy and performance indicators.

System	Description		Value	Unit
S-FO-ACH-1 or S-NG-ACH-1	Produced energy for heating	Fuel oil/gas boiler	31,472	kWh
	Produced energy for cooling	Absorption chiller	8467	kWh
		Split type air conditioners	4790	kWh
	Produced energy for DHW heating	Solar collectors	24,232	kWh
		Waste heat from ACH	4080	kWh
		Fuel oil/gas boiler	4786	kWh
	Irradiation at solar collectors		81,307	kWh
	Fuel oil/gas consumption		40,287	kWh
	Electricity consumption		4369	kWh
	ACF (absorption cooling fraction)		0.64	(-)
	SF_{DHW} (solar fraction for DHW)		0.73	(-)
	RES (renewable energy share)		0.42	(-)
S-FO-ACH-2 or S-NG-ACH-2	Produced energy for heating	Fuel oil/gas boiler	22,277	kWh
		Solar collectors	9694	kWh
	Produced energy for cooling	Absorption chiller	8466	kWh
		Split-type air conditioners	4793	kWh
	Produced energy for DHW heating	Solar collectors	14,936	kWh
		Fuel oil/gas boiler	10,037	kWh
		Waste heat from ACH	4077	kWh
	Irradiation at solar collectors		81,307	kWh
	Fuel oil/gas consumption		35,905	kWh
	Electricity consumption		4419	kWh
	ACF (absorption cooling fraction)		0.64	(-)
	SF_{H} (solar fraction for building heating)		0.30	(-)
	SF_{DHW} (solar fraction for DHW heating)		0.51	(-)
	RES (renewable energy share)		0.45	(-)
AWHP-1	Produced energy for heating		32,441	kWh
	Produced energy for cooling		12,956	kWh
	Produced energy for DHW heating		32,104	kWh
	Electricity consumption	Heat pump (building heating)	12,920	kWh
		Heat pump (building cooling)	3797	kWh
		Heat pump (DHW heating)	9024	kWh
		Auxiliary (pumps)	4333	kWh
	RES (renewable energy share)		0.59	(-)
AWHP-2	* HVAC system energy production, consumption and performance is the same as for AWHP-1 system			
	Electricity from PV		15,057	kWh
	Electricity from grid		15,018	kWh
	RES (renewable energy share)		0.79	(-)

The absorption SHC system in the proposed design operates with a high absorption cooling fraction ACF of 0.64, which means that it is used to meet the base cooling load. The thermal energy required to operate the absorption chiller (generator heating) is supplied entirely by solar thermal collectors; thus, the solar fractions for the generator of absorption cooling are not presented. The solar fraction for DHW heating SF_{DHW} is large for both variants of the absorption SHC system because of the low DHW consumption. Waste heat from the condenser and the absorber of the ACH is used for preheating the DHW, but the share of this heat in the total energy demand is small, ranging from 0.12 to 0.14. When using heat from solar thermal collectors for building heating, 30% of the required energy for heating is provided by solar collectors (S-FO-ACH-2, S-NG-ACH-2). The share of renewable energy (RES) is 0.42 (S-FO-ACH-1, S-NG-ACH-1) and 0.45 (S-FO-ACH-2, S-NG-ACH-2) and cannot be increased further without replacing nonrenewable fuel oil or natural gas in these systems with renewable sources. The RES share of the AWHP-1 system is slightly higher than previous systems (0.59), and it is further increased to 0.79 by implementing PV panels (AWHP-2 system).

The solutions considering the specific global costs and primary energy consumption are evaluated according to the Pareto concept and are presented in Figure 9. The solutions from HVAC systems and energy price scenarios can be easily distinguished, as they are grouped by primary energy consumption. Cost-optimal solutions that minimize the global cost over the predicted life cycle for all the energy price scenarios are achieved with the AWHP-2 system. This system also achieved solutions with the lowest primary energy consumption indicator PEC. Absorption SHC systems achieved high global costs due to large investment costs. The primary energy consumption of absorption SHC systems is very close to the consumption achieved with the AWHP-1 system. The use of renewable energy from solar panels for building heating reduces the primary energy consumption of these systems by 10%. The impact of high electricity prices is most visible in AWHP-1 and AWHP-2 systems, where the global costs of solutions can vary by 30%.

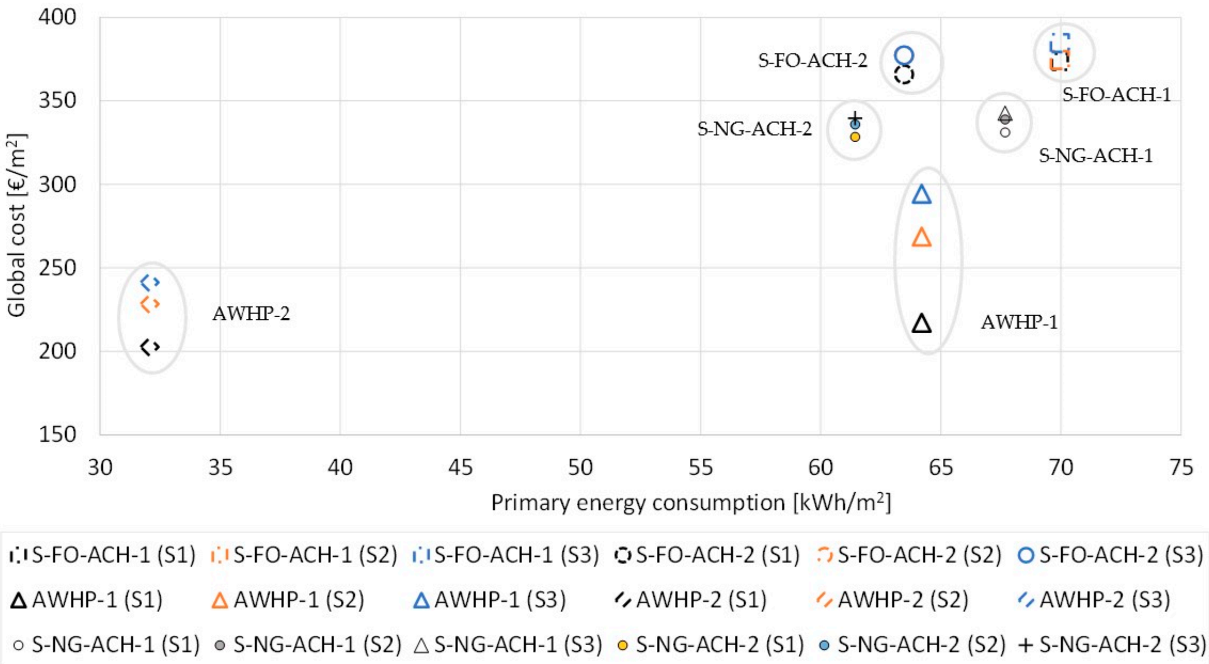

Figure 9. Results of global cost and primary energy consumption from simulations for HVAC systems in three scenarios of energy prices (S1, S2, S3).

The annual specific costs for energy and maintenance are shown in Figure 10. Maintenance costs are constant and do not differ between energy price scenarios. The price of electricity mainly affects the energy cost of AWHP systems, which consume a larger share of electricity compared to absorption SHC systems. The highest annual operation cost achieved for the AWHP-1 system is achieved in the S3 scenario with the highest electricity price. The application of the electricity production system in AWHP-2 is beneficial because it reduces both the energy price and the primary energy consumption. The advantage is visible in all three energy price scenarios. The lowest energy cost in the scenario with present energy prices is achieved with the AWHP-2 system, while in the scenarios with increased electricity prices, it is achieved with the systems that use natural gas. This leads to the conclusion that the operation of the absorption SHC system could be price competitive to the AWHP system only in the scenario with increased electricity price.

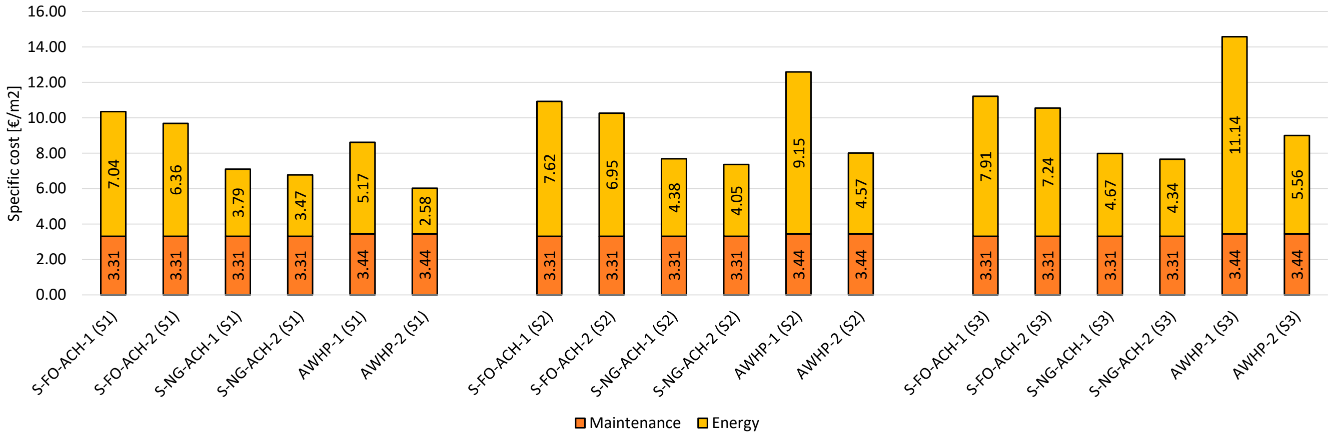

Figure 10. Maintenance and energy costs for HVAC systems operating in three scenarios of energy prices.

Electricity consumption and operation cost of the ACH with STC and split AC as well as the air-to-water heat pump in the cooling regime are extracted from the simulation data and are compared in Figure 11. Electricity consumption, primary energy consumption and operation costs are lower by 30% for the system with the ACH and split-type AC. Most of the electricity consumption in the system with the ACH makes the electricity for running circulation pumps and cooling tower fans. When the cooling-only regime is considered, the operation cost is the highest for the AWHP system.

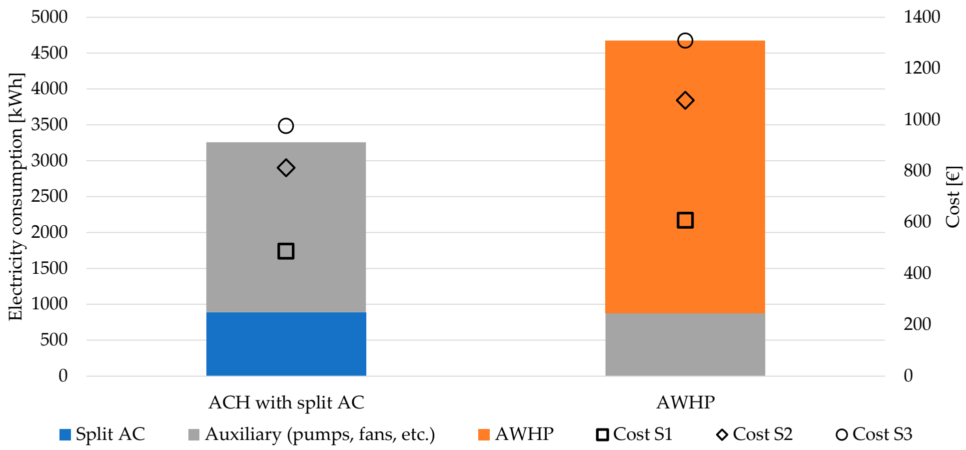

Figure 11. Annual electricity consumption (bars) and energy costs (markers) in three scenarios of energy prices for ACH with split AC and AWHP in the cooling regime.

The specific electricity consumption per kWh of produced cooling energy can be calculated by using the produced cooling energy presented earlier in Table 6, which is shown in Figure 12. The lowest electricity consumption is achieved for split AC units, while the highest is for AWHP units. Although the input energy for running the generator of the

ACH can be considered free energy, cooling by the ACH with solar thermal collectors has high electricity consumption due to a large number of auxiliary energy consumers (pumps, fans, etc.). It can be concluded that a solar thermal cooling system must have at least the same or a lower price than a comparable AWHP system to be economically viable.

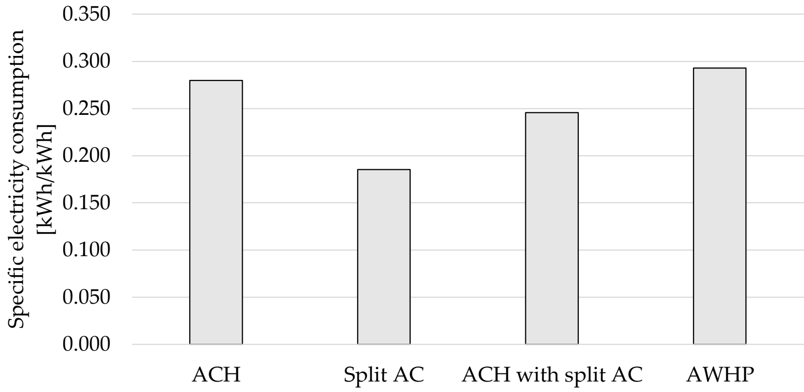

Figure 12. Specific electricity consumption per kWh of produced cooling energy with ACH, split AC, and ACH with split AC and AWHP.

CO_2 emissions are calculated from the final energy using CO_2 emission factors. The annual emissions for the systems are shown in Figure 13. Emissions are the lowest for the systems that operate with AWHP and PV modules (AWHP-2). As expected, emissions are the highest for systems with solar panels and fuel oil boilers, followed by systems with solar panels and natural gas boilers.

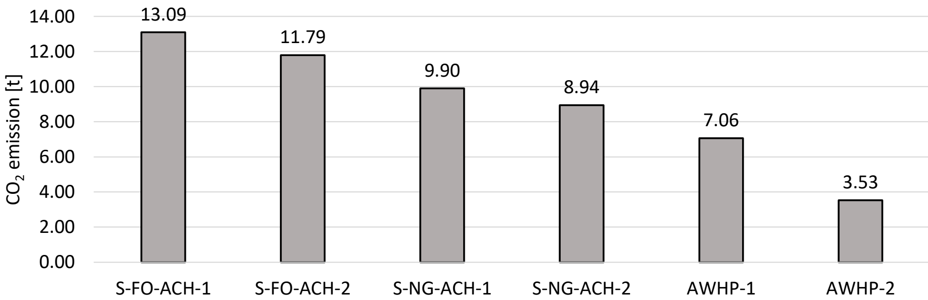

Figure 13. Annual CO_2 emissions for operation of HVAC systems.

Costs during the lifetime of HVAC systems for three scenarios of energy prices are presented in Figure 14. The investment cost is introduced in the starting year.

The lowest lifetime cost for all the energy price scenarios is achieved with the implementation of a PV plant in an AWHP-based HVAC (AWHP-2) system. The payback period for the AWHP-2 system varies depending on the price of electricity. The longest payback period of 7 years is achieved in scenario 1 with the lowest electricity price. The payback period decreases further to 3.5 years (scenario 2) and 2.5 years (scenario 3). Absorption SHC systems cannot match the lifetime costs of AWHP systems due to the higher investment costs. As mentioned earlier, these systems could only be competitive with the AWHP system in a scenario with increased electricity prices and drastically reduced investment costs for such systems. This scenario is simulated in Figure 15, using investment cost for absorption SHC systems of 80,000 EUR. In this scenario, the system S-NG-ACH-2 achieves the lowest lifetime cost.

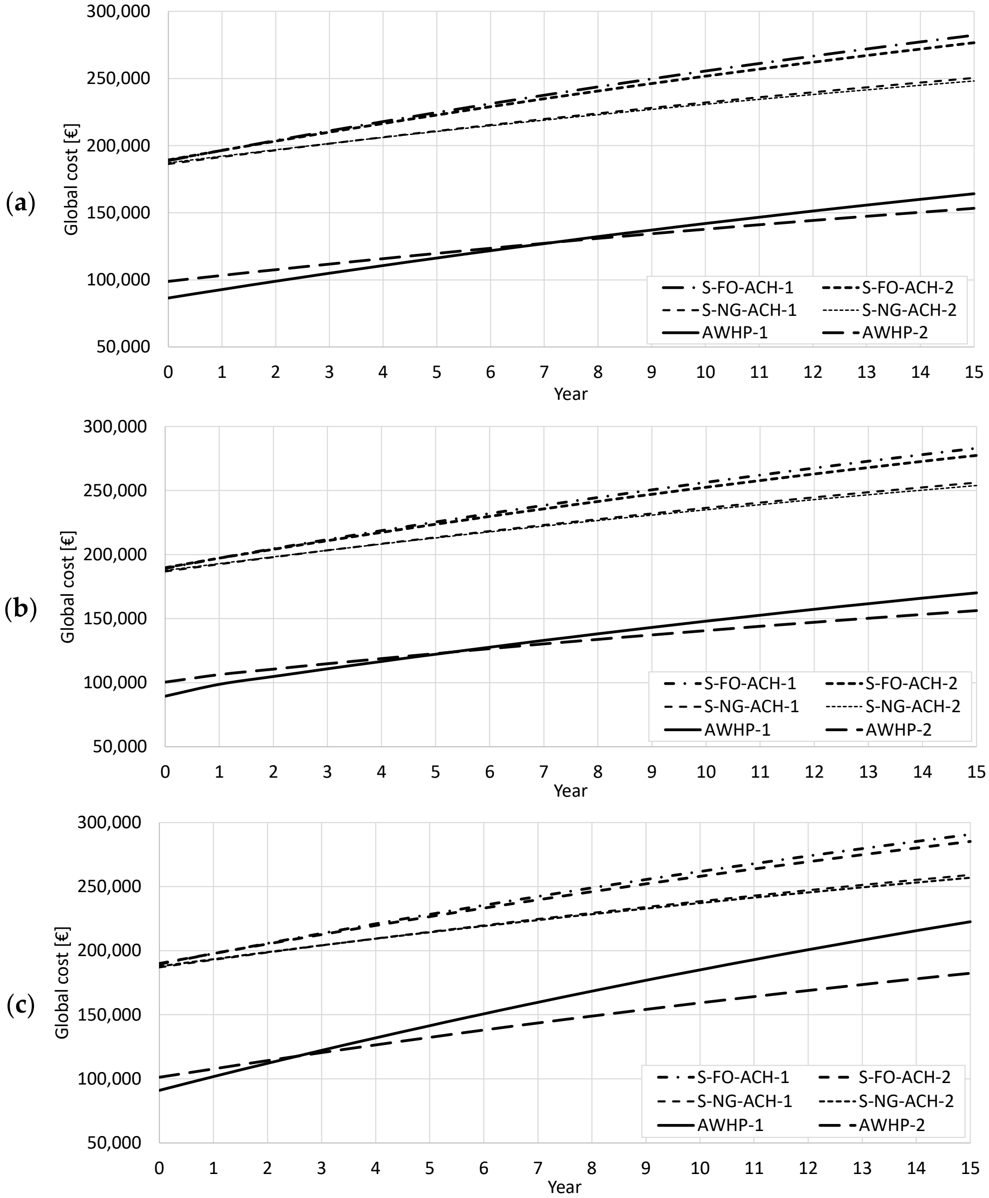

Figure 14. Lifetime costs for considered energy price scenarios: (**a**) S1, (**b**) S2, (**c**) S3.

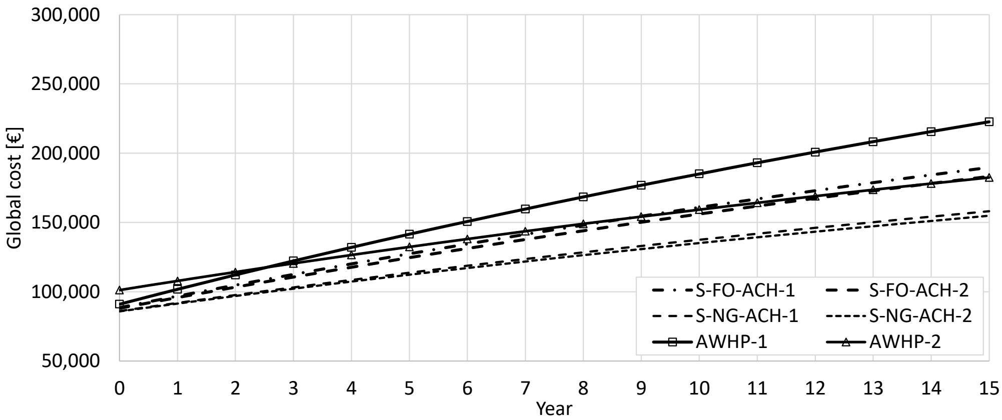

Figure 15. Lifetime costs for energy price scenario S1 and reduced investment cost for absorption SHC systems.

4. Conclusions

The study presented in this article compares different configurations of SHC systems based on solar thermal collectors, PV modules, absorption chillers and air-to-water heat pumps. Dynamic simulation models were applied to a building located in a mild Mediterranean climate. The existing SHC system with evacuated tube solar collectors and a small single-stage absorption chiller designed to cover the base cooling load was used as a reference system for the extended analysis. A full economic and energy evaluation of the system operation during its lifetime was performed for different price scenarios.

Among the considered systems, the system with the lowest primary energy consumption and lowest overall costs during the lifetime was the system with an air-to-water heat pump with PV modules sized to cover the nonrenewable part of the consumed electric energy.

Despite the significant increases in energy prices, absorption SHC systems are still not a viable solution for low-capacity applications, even in the case where all energy flows are used, such as when condenser/absorber heat is used for DHW heating or when solar heat is used directly for winter heating. Only in the case of a hypothetical reduction of the investment cost for an absorption SHC system to the level of the investment price of a grid-connected vapor compression heat pump could the absorption SHC system create favorable conditions for future use.

Author Contributions: Conceptualization, B.D. and B.P.; methodology, B.D. and B.P.; software, B.D.; validation, B.D., B.P. and V.G.; formal analysis, B.D., B.P. and V.G.; investigation, B.D. and B.P.; resources, B.D. and B.P.; data curation, B.D., B.P. and V.G.; writing—original draft preparation, B.D.; writing—review and editing, B.D., B.P. and V.G.; visualization, B.D. and B.P.; supervision, B.D. and B.P.; project administration, B.P.; funding acquisition, B.P. All authors have read and agreed to the published version of the manuscript.

Funding: This research was funded by the University of Rijeka project (uniri-tehnic-18-14).

Data Availability Statement: Not applicable.

Conflicts of Interest: The authors declare no conflict of interest.

Nomenclature

A	area (m^2)
ACF	absorption cooling fraction (-)
ACH	absorption chiller
C	cooling
CI	cost indicator (EUR/m^2)
cons	consumed
E	energy (kWh)
ee	electrical energy
f	primary energy factor (-)
G	cost (EUR)
g	global
I	investment
imp	imported
nren	nonrenewable
P	primary
PEC	primary energy consumption indicator (kWh/m^2)
prod	produced
RES	renewable energy share (-)

R_d	discount factor (-)
SF	solar fraction (-)
SOL	solar
$V_{f,\tau}$	residual value (-)
Abbreviations	
ACH	absorption chiller
AWHP	air-to-water heat pump
H/C	heating and cooling
PV	photovoltaic
STC	solar thermal collectors
SHC	solar heating and cooling
TRY	test reference year

References

1. Solar Heat Markets in Europe. 2022. Available online: http://solarheateurope.eu/publications/market-statistics/solar-heat-markets-in-europe/ (accessed on 15 December 2022).
2. Solar Heat Markets in Europe. 2021. Available online: http://solarheateurope.eu/project/solar-thermal-markets-in-europe-trends-and-market-statistics-2021-published-in-february-2022// (accessed on 15 December 2022).
3. ESTIE. Solar Thermal Markets in Europe—Trends and Market Statistics 2015. 2016. Available online: http://solarheateurope.eu/2016/11/01/solar-thermal-markets-europe-trends-market-statistics-2015-published-november-2016/ (accessed on 15 December 2022).
4. IEA. Space Cooling. 2022. Available online: https://www.iea.org/reports/space-cooling (accessed on 11 January 2023).
5. SHC Annual Report. 2018. Available online: https://shc.amegroups.com/announcement/view/128 (accessed on 15 December 2022).
6. Bellos, E.; Tzivanidis, C.; Antonopoulos, K. Exergetic, energetic and financial evaluation of a solar driven absorption cooling system with various collector types. *Appl. Therm. Eng.* **2016**, *102*, 749–759. [CrossRef]
7. Mateus, T.; Oliveira, A. Energy and economic analysis of an integrated solar absorption cooling and heating system in different building types and climates. *Appl. Energy* **2009**, *86*, 949–957. [CrossRef]
8. Eicker, U.; Pietruschka, D. Design and performance of solar powered absorption cooling systems in office buildings. *Energy Build.* **2009**, *41*, 81–91. [CrossRef]
9. Hang, Y.; Qu, M.; Zhao, F. Economical and environmental assessment of an optimized solar cooling system for a medium-sized benchmark office building in Los Angeles, California. *Renew. Energy* **2011**, *36*, 648–658. [CrossRef]
10. Calise, F.; Palombo, A.; Vanoli, L. Maximization of primary energy savings of solar heating and cooling systems by transient simulations and computer design of experiments. *Appl. Energy* **2010**, *87*, 524–540. [CrossRef]
11. Shirazi, A.; Taylor, R.; White, S.; Morrison, G. Transient simulation and parametric study of solar-assisted heating and cooling absorption systems: An energetic, economic and environmental (3E) assessment. *Renew. Energy* **2016**, *86*, 955–971. [CrossRef]
12. Eicker, U.; Pietruschka, D.; Pesch, R. Heat rejection and primary energy efficiency of solar driven absorption cooling systems. *Int. J. Refrig.* **2012**, *35*, 729–738. [CrossRef]
13. Calise, F. Thermoeconomic analysis and optimization of high efficiency solar heating and cooling systems for different Italian school buildings and climates. *Energy Build.* **2010**, *42*, 992–1003. [CrossRef]
14. Florides, G.; Kalogirou, S.; Tassou, S.; Wrobel, L. Modelling and simulation of an absorption solar cooling system for Cyprus. *Sol. Energy* **2002**, *72*, 43–51. [CrossRef]
15. Florides, G.; Kalogirou, S.; Tassou, S.; Wrobel, L. Modelling, simulation and warming impact assessment of a domestic-size absorption solar cooling system. *Appl. Therm. Eng.* **2002**, *22*, 1313–1325. [CrossRef]
16. Arsalis, A.; Alexandrou, A. Parametric study and cost analysis of a solar-heating-and-cooling system for detached single-family households in hot climate. *Sol. Energy* **2015**, *117*, 59–73. [CrossRef]
17. Tsoutsos, T.; Aloumpi, E.; Gkouskos, Z.; Karagiorgas, M. Design of a solar absorption cooling system in a Greek hospital. *Energy Build.* **2010**, *42*, 265–272. [CrossRef]
18. Eicker, U.; Pietruschka, D.; Haag, M.; Schmitt, A. Systematic design and analysis of solar thermal cooling systems in different climates. *Renew. Energy* **2015**, *80*, 827–836. [CrossRef]
19. Ma, Y.; Saha, S.; Miller, W.; Guan, L. Comparison of Different Solar-Assisted Air Conditioning Systems for Australian Office Buildings. *Energies* **2017**, *10*, 1463. [CrossRef]
20. Huang, L.; Zheng, R.; Piontek, U. Installation and Operation of a Solar Cooling and Heating System Incorporated with Air-Source Heat Pumps. *Energies* **2019**, *12*, 996. [CrossRef]
21. Figaj, R.; Żołądek, M. Operation and Performance Assessment of a Hybrid Solar Heating and Cooling System for Different Configurations and Climatic Conditions. *Energies* **2021**, *14*, 1142. [CrossRef]
22. Kaneesamkandi, Z.; Almujahid, A.; Salim, B. Selection of an Appropriate Solar Thermal Technology for Solar Vapor Absorption Cooling—An MADM Approach. *Energies* **2022**, *15*, 1882. [CrossRef]

23. Lazzarin, R.; Noro, M.; Zanni, O. Solar thermal and ground source absorption heat pump: Energy analysis for a nearly Zero Energy Building. In Proceedings of the 25th IIR International Congress of Refrigeration, Montréal, Canada, 24–30 August 2019; p. 8. [CrossRef]
24. Energy in Croatia—Annual Energy Report 2019. 2020. Available online: https://mingor.gov.hr/UserDocsImages/UPRAVA%20ZA%20ENERGETIKU/Energija_u_Hrvatskoj/Energija_u_Hrvatskoj_2019-2.pdf/ (accessed on 15 December 2022).
25. Eurostat (European Statistical Office). 2022. Available online: https://ec.europa.eu/eurostat (accessed on 26 January 2022).
26. Soldo, V.; Novak, S.; Horvat, I. *Algorithm for Calculating the Energy Required for Heating and Cooling Building Space According to HRN EN ISO 13790*; University of Zagreb, Faculty of Engineering: Zagreb, Croatia, 2017.
27. Meteonorm. *Meteonorm—Global Meteorological Databa*; Meteotest: Bern, Switzerland, 2012.
28. Technical Regulation on Rational Use of Energy and Thermal Protection in Buildings, Croatia. 2015. Available online: https://narodne-novine.nn.hr/clanci/sluzbeni/dodatni/438515.pdf (accessed on 15 December 2022).
29. *EN 12831*; Energy Performance of Buildings—Method for Calculation of the Design Heat Load. BSI Standards: Brussels, Belgium, 2017.
30. *Richtlinie VDI 2078 Blatt 1 Berechnung der Kühllast klimatisierter Gebäude bei Raumkühlung über Raumumschließungsflächen*; Bauphysik: Berlin, Germany, 2003. [CrossRef]
31. Recknagel, E.; Sprenger, H.; Schramek, E.-R. *Taschenbuch fur Heizung und Klimatechnik*; Oldenbourg Industrieverlag: Munchen, Germany, 2007.
32. Delač, B. *Optimization of Energy Systems for Nearly Zero Energy Buildings Using Dynamic Simulations*; Faculty of Engineering, University of Rijeka: Rijeka, Croatia, 2017.
33. Commission Delegated Regulation No 244/2012. 2012. Available online: http://www.buildup.eu/sites/default/files/content/l_08120120321en00180036.pdf (accessed on 15 December 2022).
34. *Guidelines Accompanying Commission Delegated Regulation (EU) No 244/2012 of 16 January 2012 Supplementing Directive 2010/31/EU of the European Parliament and of the Council (2012/C 115/01)*; EU: Brussels, Belgium, 2012.